The effect of phosphorus on manganocolumbite and mangaotantalite solubility in peralkaline to peraluminous granitic melts

TANG YONG[a, b], ZHANG HUI[a, *], RAO BING[b]

[a]Key laboratory of High-temperature and High-pressure Study of the Earth's Interior, Institute of Geochemistry, Chinese Academy of Sciences, Guiyang 550081, China

[b]State Key Laboratory of Ore Deposit Geochemistry, Institute of Geochemistry, Chinese Academy of Sciences, Guiyang 550081, China.

ABSTRACT

Solubility experiments of Mn-columbite ($MnNb_2O_6$) and Mn-tantalite ($MnTa_2O_6$) were conducted under water saturated conditions in synthetic haplogranitic melts containing different amounts of phosphorus at 800 °C and 100 MPa. All experiments were carried out in cold-seal rapid quenching pressure vessels (RQV) with water as a pressure medium. Experimental results show that: 1) the solubilities of $MnNb_2O_6$ and $MnTa_2O_6$ in peralkaline melts are higher than those in peraluminous melts; 2) phosphorus has strong influence on the solubilities of $MnTa_2O_6$ and $MnNb_2O_6$ in peralkaline melts, K_{Sp}^{Nb} and K_{Sp}^{Ta} decrease from 104.89×10^{-4} mol^2/kg^2 and 107.62×10^{-4} mol^2/kg^2 for melts without P_2O_5 to 16.11×10^{-4} mol^2/kg^2 and 7.96×10^{-4} mol^2/kg^2 for melts containing ~4.00 wt.% P_2O_5, respectively; 3) phosphorus has less influence on the solubilities of $MnTa_2O_6$ and $MnNb_2O_6$ in peraluminous melt, K_{Sp}^{Nb} decrease from 4.50×10^{-4} mol^2/kg^2 for melts without P_2O_5 to 0.73×10^{-4} mol^2/kg^2, and K_{Sp}^{Ta} from 3.57×10^{-4} mol^2/kg^2 to 0.14×10^{-4} mol^2/kg^2 for melts contaning ~5.00 wt.%

P_2O_5. Taking the structural role of phosphorus into account, P decreases the solubility of Mn-columbite and Mn-tantalite via competing for network modifiers.

Keywords: Columbite, Tantalite, solubility, Phosphorus, melt

INTRODUCATION

Niobium (Nb) and Tantalum (Ta) almost always occur together in nature. Both of them are key metals in high technology industries. Nb is a ductile metal with a high melting point, relatively low density properties, so it is usually used to manufacture high-strength low-alloy steels. Ta is often applied to electronics industry due to its unique ability to store and release energy. The columbite-tantalite group (Fe, Mn)(Ta, Nb)$_2O_6$ is one of the most economically important Nb-Ta-containing minerals. These minerals are generally concentrated in rare-metal peraluminous granites and pegmatites, which are typically enriched in fluxing elements such as H_2O, Li, F, P and B. The solubility of Nb-Ta-containing minerals in parental melts is considered to be a fundamental parameter to control the potential formation of Ta-Nb ore deposits. For these reasons, knowledge of the effect of fluxing elements on the solubility of the Nb-Ta-containing mineral group in silicate melts is crucial in understanding the formation of Nb-Ta deposits. Data on the effects of H_2O on the solubility of Mn(Ta, Nb)$_2O_6$ have been published by Linnen (2005) and indicated that for melts containing more than approximately 1 wt.% H_2O, the water does not affect these minerals solubility. Linnen (1998) showed that the solubilities of columbite and tantalite increase with Li content in water-saturated granitic melt. Keppler (1993) reported that

the solubilities of columbite and tantalite increases with increasing F content in the melt, but the later experiments suggest that F has only weak or no effect on the solubility of tantalite and columbite (Van Lichtervelde et al. 2010; Fiege et al. 2011; Aseri et al. 2015).

In addition to H_2O, Li and F, P is also the key element involving Nb and Ta mineralization. Many Nb-Ta deposits are P-rich character, such as the beryl-columbite-phosphate pegmatite and rare metal granite (e.g., Nanping No.31 Nb-Ta deposits, China, Rao et al. 2014; Yichun 414 Nb-Ta deposits, China, Yin et al. 1995; Beauvoir granite, France, Raimbault et al. 1995). Bartels et al. (2010) observed an increase of the solubility of columbite and tantalite with increasing amounts of fluxing elements including Li, F, B and P. Although these experiments were useful in interpreting the general effect of increasing amounts of fluxing elements, they were not suited for determination of individual effect of P. Wolf and London (1993) suggested that phosphorus may increase the solubilities of columbite and tantalite, whereas, Aseri et al. (2015) concluded that P can apparently decrease the solubilities of columbite and tantalite by competition for network-modifier cations. In order to resolve the conflicting results about the effect of P on columbite and tantalite, a series of experiments were completed with various melt compositions, ranging from peralkaline to peraluminous.

METHOD

Starting glass

The starting glasses were synthesized from reagent grade oxides and carbonates (high purity SiO_2, Al_2O_3, Na_2CO_3, K_2CO_3,). Phosphorus was added in the form of

$[NH_4]H_2PO_4$. The powders were mixed and ground in agate mortars. Mixtures were melted in platinum crucibles at 1,500 °C using an electric furnace with molybdenum silicide heating elements, and fusion time was limited to one hour to minimize alkali loss. The platinum crucibles were then removed quickly and placed in a water tank for fast quenching. In order to generate homogeneous glasses, this process of grinding, fusing, and rapid quenching, was repeated 2 to 3 times for each starting compositions. A chip of starting glass was mounted in epoxy, and homogeneity of this glass was checked by WDS X-ray maps of K, Na, Al, P, and Si using electron microprobe. The compositions of the power of the starting glasses determined by XRF are listed in Table 1.

Starting minerals

In accordance with earlier studies (Linnen and Keppler 1997), the Mn end-members of $(Fe, Mn)(Ta,Nb)_2O_6$ were selected for this study because significant According to Robie et al. (1995), Mn^{3+} occurs only at very high oxygen fugacity and thus fO_2 does not need to be carefully controlled. Mn-columbite ($MnNb_2O_6$) and Mn-tantalite ($MnTa_2O_6$) were synthesized hydrothermally by sealing 500 mg of a stoichiometric oxide mixture plus 50 mg of 5% HF solution in Au capsules (length 50, i.d. 3.8, o.d. 4.0 mm), then placing the capsules in H_2O pressurized Rapid Quench Vessel (RQV) at 800 °C and 100 MPa for 10 days. The crystals are 3~11 μm, and fully ordered manganocolumbite (Mn-columbite) or manganotantalite (Mn-tantalite) were the only phases identifiable from X-ray powder diffraction patterns after the syntheses. Analyzed by electron microprobe (EMP), the totals of the crystals are about 100 wt.%, and the average Mn/Nb and Mn/Ta molar ratios are 0.52 and 0.49, respectively, as expected for Mn-columbite and Mn-tantalite. The results of the EMP analyses are listed in Table2.

High temperature and pressure solubility experiments

All runs were conducted in cold-seal rapid quench pressure vessels at 800°C and 100MPa with run durations between 10 and 16 days. The run temperature and pressure were measured by PtRh-Pt thermocouple and Bourdon-tube pressure gauge with errors of 1°C and 5 MPa, respectively. The oxygen fugacity was not strictly buffered, however, the Ni-Cr alloy of the vessel (made of GH220, commensurate with René-41) and H_2O as pressure medium impose an oxygen fugacity upon the system which is close to Ni-NiO (Chou 1987).

Approximately 200 mg of starting glass and 20 mg of $MnNb_2O_6$ and $TaNb_2O_6$ were gently mixed, and then loaded into an Au capsule (length 50, i.d. 3.8, o.d. 4.0 mm) containing 10~15 mg of distilled H_2O. The loaded capsule was welded shut by an oxygen-acetylene flame, placed in a drying oven at 120 °C, and then checked for weight loss. The capsule was inserted into the pressure vessel which was put into a horizontal tubular electric furnace. After the experiments, the pressure vessel was withdraw from the furnace and titled upwards (at 90° angle from horizontal), and the Au capsule slid into quenching part of vessel and then was quenched isobarically from 800°C to ambient temperature in several seconds. Small chips of run productions were taken from the Au capsule, and analyzed by electron microprobe.

Analytical methods

Glass compositions were determined at the State Key Laboratory of Geological Processes and Mineral Resources, China University of Geosciences (Wuhan), using a JEOL JXA-8100 Electron Probe Micro Analyzer equipped with four

wavelength-dispersive spectrometers (WDS). An accelerating voltage of 15 kV, a beam current of 2 nA and a 20 μm beam diameter, which recommended by Morgan and London (1996) to minimize the Na loss during the measurement, were used to analyze Na, K, Al and Si, and followed by a 20 nA for analysis of Nb, Ta, Mn and P. The counting time for Na, K, Al and Si was 10s, and for all other elements was 60s. The standards were jadeite for Na and Si, garnet for Al, sanidine for K, niobium metal for Nb, Tantalum metal for Ta, rhodonite for Mn and apatite for P. Data were corrected on-line using a modified ZAF (atomic number, absorption, fluorescence) correction procedure. The water contents of the glass were estimated based on difference of EMPA oxide totals from 100%.

RESULT

All solubility experiment products were glasses, few bubble and crystals of investigated minerals and no other phases were observed. The sizes of Mn-columbite and Mn-tantalite crystals in the run products range from <1 μm to 20 μm (Fig. 1). The concentrations of Nb, Ta and Mn were analyzed by EMP, and the analytical spots are randomly selected, close to or far away from theses crystals. The acquired concentrations of Nb, Ta and Mn from different spots coincide within errors in individual run product, implying that these elements distribute homogeneously in glass. The ultimate results are given in Table 3 and Appendix A. The Mn-columbite and Mn-tantalite are assumed to dissociate into oxides in the melt, as discussed by the previous researchers (e.g., Linnen and Keppler 1997):

$$MnNb_2O_6^{\ crystal} = MnO^{\ melt} + Nb_2O_5^{\ melt}$$

159 $MnTa_2O_6$ ^{crystal}= MnO ^{melt} + Ta_2O_5 ^{melt}

160 The equilibrium between melt and solid Mn-columbite or Mn-tantalite can be
161 described by the solubility products:

162 K_{Sp}^{Nb} (mol^2/kg^2) = X (MnO) (mol/kg) × X (Nb_2O_5) (mol/kg)

163 K_{Sp}^{Ta} (mol^2/kg^2) = X (MnO) (mol/kg) × X (Ta_2O_5) (mol/kg)

164 Where X represents the molar concentration of MnO, Nb_2O_5 and Ta_2O_5 in the melt.

165 As shown in Fig. 2, the phosphorus has a major influence on the solubility of
166 columbite-tantalite in the peralkaline melt. In these melt compostions, there is a
167 negative dependence of solubilities of Mn-columbite and Mn-tantalite on the
168 phosphorus content. K_{Sp}^{Nb} and K_{Sp}^{Ta} decrease from 104.89±6.55 $\times10^{-4}$ mol^2/kg^2 and
169 107.62±18.84 $\times10^{-4}$ mol^2/kg^2 for melts without P_2O_5 to 16.11±4.65$\times10^{-4}$ mol^2/kg^2 and
170 7.96±1.60$\times10^{-4}$ mol^2/kg^2 for melt containing ~4.0 wt.% P_2O_5, respectively; By
171 contrast, the phosphorus has a less influence on the solubilities of $MnTa_2O_6$ and
172 $MnNb_2O_6$ in peraluminous composition, K_{Sp}^{Nb} decrease from 4.50±1.85$\times10^{-4}$
173 mol^2/kg^2 for melt without P_2O_5 to 0.73±0.40$\times10^{-4}$ mol^2/kg^2 for melt containing
174 ~5wt.%, and K_{Sp}^{Ta} from 7.96±1.60$\times10^{-4}$ mol^2/kg^2 to 0.14±0.07$\times10^{-4}$ mol^2/kg^2.

175 **DISCUSSION**

176 **Criteria for equilibrium**

177 The attainment of equilibrium is extremely important in solubility experiments.
178 Theoretically, the experimental duration must be long enough to allow the elements
179 derived from the crystals of investigated minerals to diffuse completely throughout
180 the melt. At the same pressure and temperature, metaluminous melts are more viscous

than both peraluminous and peraluminous (Toplis and Dingwell 1996); and the diffusivity of Ta is close to or slower than that of Nb in the melt (Mungall et al. 1999; Bartels et al., 2010). So the equilibrium experiments of Mn-tantalite in metaluminous were conducted for different run durations (TA9 for 10 days and Ta9[1] for 16), and the calculated solubility products are identical within error (Table 3). These results indicate that the run duration of 10 days used in the present work is sufficient to reach equilibrium conditions.

The equilibrium can be tested by the molar Mn/Nb and Mn/Ta ratios in products (Bartels et al. 2010). If the dissolution of Mn-columbite and Mn-tantalite is congruent just like reactions as given above, the molar Mn/Nb and Mn/Ta ratios are equal to the stiochiometric values of Mn-columbite and Mn-tantalite (~0.5). For most experiments, The Mn/Nb and Mn/Ta ratios are very close or equal to 0.5, which is evidence for equilibrium between melt and these minerals. Further, K_{sp}^{Nb} and K_{sp}^{Ta} for P-free melt are very close to the reference curve of Linnen and Keppler (1997) (Fig. 3), also supporting attainment of equilibrium.

However, non-stiochiometric Mn/Ta ratios also exist. The problematic experiment is Ta2, and and the Mn/Ta ratios is 1.24±0.15. Non-stiochiometric Mn/Ta ratios are also encountered by the previous researchers, and some mechanisms are proposed, such as, non-equilibrium resulted from the slow diffusivity of Ta relative to Mn (Aseri et al. 2015), crystallization of new Ta-bearing minerals (e.g., (Na, $K)_2Si_2Ta_2(OH)_7$ and $NaTaO_3$, Linnen and Keppler 1997; $Al_4Ta_3O_{13}(OH)$, Van Lichtervelde et al. 2010) and the possible excesses of Mn in synthetic Mn-tantalite

(Linnen and Keppler 1997). As discussed above, no additional crystallization phase was identified in the run products, and the equilibrium experiments indicate that the run duration of 10 days lasting in the present work is sufficient to reach equilibrium conditions. Therefore, possible excesses of Mn in synthetic Mn-tantalite account for the large Mn/Ta ratios in these melts. The presence of excess Mn does not apparently affect the equilibrium values according to the experiments using initially doping glasses with Mn (Linnen and Keppler 1997).

The effect of phosphorus

The solubilities of high field-strength cations in high silica melts strongly depend on the availability of network modifiers (Watson 1979; Dickinson and Hess 1985; Ellison and Hess 1986; Hess 1991;). In order to model Mn-columbite and Mn-tantalite, it is necessary to define a parameter that reflects variations of network modifiers in silicate melts. The amount of network modifiers in melts can be obtained after subtraction of the proportion of metal cations necessary for charge-balance of Al, so it is simple to express the amount of network modifier in terms of the mol/kg values of Na+K-Al in haplogranitic melts. The mol/kg values of Na+K-Al are simplified by excess alkali (EA) and are listed in Table 3.

Fig. 3a and Fig.3b shows the solubilities of Mn-columbite and Mn-tantalie plotted against EA. The EA values of the present work form clusters. The data of P-free melt are very close to the reference curve of Linnen and Keppler (1997), whereas the data of P-bearing melt, especially P-rich melt, are lower than that of Linnen and Keppler (1997). The experimental results confirm that phosphorus apparently decreases the solubilities of Mn-columbite and Mn-tantalie. In order to

226 understand the effect of phosphorus on the solubilities of Mn-columbite and
227 Mn-tantalite, one first has to consider the structural role of P in haplogranitic melt in
228 absence of Nb and Ta.

229 In peralkaline melts, it is generally agreed that P essentially reacts with network
230 modifiers to form phosphate complexes, such as M_3PO_4, and $M_4P_2O_7$ or MPO_3 (M=
231 network modifier) (Gan and Hess 1992; Toplis and Dingwell 1996). Taking the
232 structural role of P into consideration, the EA should be replaced by EA_P. It is more
233 reasonable to consider Mn^{2+} to be a network modifier, just similar to the structural
234 roles of Fe and Mg (Acosta-Vigil et al. 2003), so the effective excess alkali EA_P is
235 expressed by the mol/kg Na+K+2Mn-Al-1/nP (where n is the ratio of P/M, in the
236 present work, M= Na, K and Mn). As shown in Fig.3a and 3b, if we want the
237 solubilities of Mn-columbite and Mn-tantalite in P-enrichment melts to close or fit to
238 the reference curve of Linnen and Keppler (1997), the mol/kg of network modifiers
239 should be appropriately reduced. Essentially, the reduction amount of network
240 modifiers that has to be bound to P is estimated by the horizontal distance of each
241 point to the curve. Further, the P/M ratios can be calculated and the phosphate species
242 in the peralkaline melts are predicted using these ratios. Taking the experiment Ta2 as
243 an example, the EA_{Mn} in this melt is 0.94 mol/kg (not considering the structural role
244 of P, but Mn^{2+} as a network modifier), and the EA_{LK} that coincides with reference
245 curve is approximately 0.60 mol/kg, consequently the difference between them is
246 about 0.34 mol/kg. The difference implies that the concentrations of network
247 modifiers interacting with P are ~0.34 mol/kg. The concentration of P in Nb2 is 0.13
248 mol/kg (0.91 wt.%), thus the P/M ratio of the phosphate specie in this melt is about
249 1/3 (0.13/0.34), the predicting phosphate specie might be M_3PO_4.

250 As shown in Fig. 3e and 3f , if we consider the structural role of P discussed as

above, the K_{sp}^{Nb} and K_{sp}^{Ta} gained from our experiments is close or fit to reference curve of Linnen and Keppler (1997), Our results clearly show that phosphorus decreases the solubilities of Mn-columbite and Mn-tantalite via competing for network modifiers in peralkaline melt.

The structural role of P is more complex in peraluminous melts than that in prealkaline melts, even though there is only one phosphate complex in peraluminous. In peraluminous melts, P prefers to interact with Al to form the $AlPO_4$ complex (Mysen et al. 1997; Wolf and London 1994). The Al that participates in the formation of $AlPO_4$ units comes from two distinct structural positions. One is where excess Al acts as network modifier (Mysen and Toplis, 2007; Thompson and Stebbins, 2011). In this case, P reacts with excess Al and reduces the available network modifiers in the melt, and therefore reduces the solubilities of Mn-columbite and M-tantalie. This above mechanism is illustrated in the Fig.2d, and the K_{sp}^{Nb} and K_{sp}^{Ta} decrease with the increasing of P concentration in melts. In this case, the role of P in affecting the solubilities of Mn-columbite and Mn-tantalie in peraluminous is similar to that in peralkaline melts.

In the second case, when the total amount of P exceeds the amount of excess Al in the highest P-rich melt, P will also interact with Al that is charge-balanced with network-modifiers. This mechanism results in the increase of network modifiers as illustrated with the following schematic equations (Mysen et al., 1997):

$2MAlSi_3O_8+P_2O_5=AlPO_4+2MSi_3O_9$. (M= Na, K, and Mn in the present work)

Therefore this mechanism will slow down the decreasing trend of the solubilities of Mn-columbite and Mn-tantaliem, and may account for the almost same K_{sp}^{Nb} of the melt containing ~ 5 wt.% P_2O_5 as the data of melt containing ~ 3 wt.% P_2O_5.

IMPLICATIONS

Holtz et al. (1993) identified by experiments that H_2O solubility in granitic melt increases with increasing F, B and P. London (2009) further point out that first, the addition of B, P, or F increase the isobaric-isothermal solubility of H in a granitic melt; second, a melt-speciation reaction M^+A (M=metal cation, A=B, F, or P)+H^+=H^+A+M^+ happen and is shifted to the right as the activity of H^+ in the melt increases; third, the dissolution of H_2O into granitic melt, and the diffusion of H and of O is uncouple. H^+ in the melt acts as charge-balancing cation similar to those of any other network modifier. Therefore, H^+ can also interact with Al (cf. Acosta-Vigil et al., 2012).

We do not consider the effect of water on the solubilities of Mn-columbite and Mn-tantalite in the present work due to the following reason:

a) F, B, P and even Al all can change the activity of H in the melt;

b) The solubilities of Mn-columbite and Mn-tantalite appears to be independent on water content at concentrations greater than ~2 wt.% H_2O (Linnen, 2005);

c) All experiments are water saturation and contain > 2wt.% H_2O, ranging from 4.20 to 5.34 wt.%.

Fig. 4a and Fig.4b shows the correlation of $-\log K_{sp}$ and EA. Except for the melt containing single P, other K_{sp}^{Nb} and K_{sp}^{Ta} gained from flux-elements-rich melt are higher than those of Linnen and Keppler (1997), whereas if taking the structural role of fluxing elements like Li, and P into account, most of the product data are close or fit the reference curve of Linnen and Keppler (1997) (Fig.3c and Fig.3d). These solubility data imply that:

297 1) Lithium can increase the solubility of Mn-columbite and Mn-tantalite through
298 acting as a network modifier (Linnen 1998);
299 2) Phosphorus apparently decreases the solubility of Mn-columbite and
300 Mn-tantalite via competing for network modifiers;
301 3) The effect of F on the solubilities of Mn-columbite and Mn-tantalite is still
302 ambiguous. The solubilities of Mn-columbite and Mn-tantalite are higher in F-rich
303 systemsthan those of Linnen and Keppler (1997). However, the directions of
304 increasing the solubilities of Mn-columbite and Mn-tantalite with increasing F are
305 different, some is horizontal to EA_p and others are vertical to EA_p. F can link
306 simultaneously with Al, Si and Na in silicate melt (Liu and Nekvasil 2002). The
307 complex solubility mechanism and structural role of F in aluminosilicate melt hinder
308 us to consider the effect of F on on the solubilities of Mn-columbite and Mn-tantalite.
309 The peraluminous and peralkaline melts enriched in fluxing elements are
310 candidates for the mineralization of Nb and Ta, because of their high solubilities in
311 these melts. Columbite-tantalite is typically magmatic mineral in LCT type pegmatite
312 (e.g. Tanco, Canada) or highly evolved peraluminous granites (e.g. Beauvoir, France).
313 The experiments in this study were conducted at 800°C. At this temperature, the Nb
314 and Ta concentrations required for columbite-tantalite saturation are in the range of
315 several thousand parts per million. Such Nb and Ta concentrations in natural
316 peraluminous melts are unreasonably high. For example, the Ta concentrations in
317 Beauvoir do not exceed 300 ppm (Raimbault 1995), and the bulk Ta at Tanco is also
318 estimated at about 300 ppm (Stilling et al. 2006). This would seem to require that the

Nb and Ta oxide cannot precipitate from melts as primary phase. However, Ta and Nb mineralization is always considered as a magmatic process, not a hydrothermal one in pegmatites and rare-element granites (Linnen and Cuney 2005), the dilemma can be resolved, however, if pegmatite-forming magmas crystallize at temperature well below their equilibrium solidus (London, 2008), because the solubilites of the Nb-Ta oxides in melt are strongly temperature dependent, apparently decreasing with temperature decrease (Linnen and Keppler 1997; Linnen 1998; Bartels et al. 2010; Van Lichtervelde et al. 2010; Fiege et al. 2011; Aseri et al. 2015). Most pegmatites experience undercooling upon emplacement, as a result the pegmatite dike margins will cool quickly to 425°C~500°C in this process (London, 2008). Based on the solubility data from Linnen and Cuney (2005), the temperatures of Nb and Ta oxide saturation in Tanco pegmatite calculated by London (2015) are ~525°C and ~475°C, respectively. Such low crystallization temperature can be sufficient to bring peraluminous melts to saturation in Nb and Ta oxides.

According to our experimental results, an alternative possibility can be proposed. During pegmatite formation, abrupt changes in composition can occur via the formation of chemically distinct boundary layers (London 2005; 2008). The one of factors that controls the pile-up of the excluded components in the boundary layers is their diffusivities in melt. The extreme P concentration (>40 wt% P_2O_5) in melt inclusions in quartz from pegmatite in the Erzgebirge region of southeastern Germany were described by Thomas et al. (1998). London (1998; 2014; 2015) propose that these rare and anomalously high P contents could result from the slow diffusion of P

in melts, and locally rapid growth of feldspar or especially quartz could create a boundary layer that achieves very local saturation in P, and the phosphate-rich inclusions are not represent the bulk melts that quartz are crystallized from. At 800°C, the diffusion coefficients (D) of P and B in granitic melt are 1.90×10^{-13} m^2/s and 5.57×10^{-12} m^2/s respectively (London 2009). The B-rich boundary layer is documented in relevant crystal growth experiments (London 2005). The P should be easier to pile up in boundary layers because of the slower diffusivity relative to B. Indeed, P-rich boundary layer did form adjacent to skeletal crystals of K-feldspar, when these phases crystallized from melt (Morgan and London 2005). The diffusivities of Nb and Ta are the slowest of all, such as the diffusion coefficient of Nb in granitoid melts added 3.7 wt.% H_2O is 7.84×10^{-16} m^2/s (Mungall et al. 1999). The Nb and Ta can precipitate in this situation, on the one hand, it is because Nb and Ta concentrations increase dramatically via boundary layer processes due to the slow diffusion; on the other hand, the fluxing elements like Li ($D=2.6\times10^{-7}$ m^2/s at 800°C in obsidian composition melt, Jambon and Semet 1978) and F ($D=1.92\times10^{-10}$ m^2/s, London, 2009), which increase the Nb and Ta solubility in melt, diffuse too fast to pile up in the boundary layer, whereas fluxing element P that decrease the solubility can be enriched because of the slow diffusion. Boundary layer may be brought to Nb and Ta saturation via increasing the relative concentrations of Nb and Ta, reducing the fluxing elements like F and Li, and enriching P.

Nb and Ta are highly soluble in peralkaline melts, weight percent abundance of Nb and Ta are predicated for columbite-tantalite saturation. The previous data indicate

that columbite-tantalite saturation of natural peralkaline melt is unlikely, pyrochlore rather than columbite-tantalite occur as the primary Nb-Ta minerals in these rock (Mccreath et al. 2013; Linnen et al. 2014), but on the basis of our experimental results, the precipitation of columbite-tantalite in the prealkaline melt containing high P contents become likely, because of the low solubilities of Nb and Ta in P-richened peralkaline melt.

ACKNOWLEDGEMENTS

We sincerely thank Associate Editor Dr. David London, reviewer Dr. Robert Linnen and another anonymous reviewer for their constructive and helpful reviews. We think Yang Shuiyuan for help with EMPA. The work was financially supported by Chinese National Natural Science Foundation (40903027 and 41373024) and Opening Foundation of State Key Laboratory of Ore Deposit Geochemistry, Institute of Geochemistry, CAS (201307).

References

Acosta-Vigil, A., London, D., Morgan, G., and Dewers, T. (2003) Solubility of excess alumina in hydrous granitic melts in equilibrium with peraluminous minerals at 700-800 °C and 200 MPa, and applications of the aluminum saturation index. Contributions to Mineralogy and Petrology, 146(1), 100-119.

Acosta-Vigil, A., London, D., and Morgan Vi, G.B. (2012) Chemical diffusion of major components in granitic liquids: Implications for the rates of homogenization of crustal melts. Lithos, 153, 308-323.

385 Aseri, A.A., Linnen, R.L., Che, X.D., Thibault, Y., and Holtz, F. (2015) Effects of
386 fluorine on the solubilities of Nb, Ta, Zr and Hf minerals in highly fluxed
387 water-saturated haplogranitic melts. Ore Geology Reviews, 64(0): 736-746.
388 Bartels, A., Holtz, F., and Linnen, R.L. (2010) Solubility of manganotantalite and
389 manganocolumbite in pegmatitic melts. American Mineralogist, 95(4):
390 537-544.
391 Chou, I.M. (1987) Oxygen buffer and hydrogen sensor technique at elevated pressures
392 and temperatures. in “Hydrothermal experiments techniques”. HL Barnes &
393 GC Ulmer, eds. Wiley, New York.
394 Dickinson Jr, J.E., and Hess, P.C. (1985) Rutile solubility and titanium coordination in
395 silicate melts. Geochimica et Cosmochimica Acta, 49(11), 2289-2296.
396 Ellison, A.J., and Hess, P.C. (1986) Solution behavior of +4 cations in high silica
397 melts: petrologic and geochemical implications. Contributions to Mineralogy
398 and Petrology, 94(3), 343-351.
399 Fiege, A., Kirchner, C., Holtz, F., Linnen, R.L., and Dziony, W. (2011) Influence of
400 fluorine on the solubility of manganotantalite ($MnTa_2O_6$) and
401 manganocolumbite ($MnNb_2O_6$) in granitic melts -- An experimental study.
402 Lithos, 122(3-4): 165-174.
403 Gan, H., and Hess, P.C. (1992) Phosphate speciation in potassium aluminosilicate
404 glasses. American Mineralogist, 77(5-6): 495-506.
405 Hess, P. (1991) The Role of High Field Strength Cations in Silicate Melts. In L.
406 Perchuk, and I. Kushiro, Eds. Physical Chemistry of Magmas, 9, p. 152-191.

Springer New York.

Holtz, F., Dingwell, D.B., and Behrens, H. (1993) Effects of F, B_2O_3 and P_2O_5 on the solubility of water in haplogranite melts compared to natural silicate melts. Contributions to Mineralogy and Petrology, 113(4), 492-501.

Jambon, A., and Semet, M.P. (1978) Lithium diffusion in silicate glasses of albite, orthoclase, and obsidian composition: An ion-microprobe determination. Earth and Planetary Science Letters, 37(3), 445-450.

Keppler, H. (1993) Influence of fluorine on the enrichment of high field strength trace elements in granitic rocks. Contributions to Mineralogy and Petrology, 114(4): 479-488.

Linnen, R.L. (1998) The solubility of Nb-Ta-Zr-Hf-W in granitic melts with Li and Li + F; constraints for mineralization in rare metal granites and pegmatites. Economic Geology, 93(7): 1013-1025.

Linnen, R.L. (2005) The effect of water on accessory phase solubility in subaluminous and peralkaline granitic melts. Lithos, 80(1-4): 267-280.

Linnen, R.L., and Cuney, M. (2005) Granite-related rare-element deposits and experimental constrains on Ta-Nb-W-Sn-Zr-Hf mineralization. In Linnen R.L. and Samson I.M (Eds). Rare-element Geochemistry and Mineral Deposit. Geological association of Canada, Short Course Notes, 17: 45-68.

Linnen, R.L., and Keppler, H. (1997) Columbite solubility in granitic melts: consequences for the enrichment and fractionation of Nb and Ta in the Earth's crust. Contributions to Mineralogy and Petrology, 128(2): 213-227.

Linnen, R.L., Samson, I.M., Williams-Jones, A.E., and Chakhmouradian, A.R. (2014) 13.21 - Geochemistry of the Rare-Earth Element, Nb, Ta, Hf, and Zr Deposits. In Holland, H. and Turekian, K. (Eds). Treatise on Geochemistry (Second Edition), p. 543-568. Elsevier, Oxford.

Liu, Y., and Nekvasil, H. (2002) Si-F bonding in aluminosilicate glasses: Inferences from ab initio NMR calculations. American Mineralogist, 87(2-3): 339-346.

London, D. (1998) Phosphorus-rich peraluminous granites. Acta Universitatis Carolinae-Geologica, 42, 64-68.

London, D. (2005) Granitic pegmatites: an assessment of current concepts and directions for the future. Lithos, 80(1-4), 281-303.

London, D. (2008) Pegmatites. Mineralogical Association of Canada, Special publication 10, Quebec.

London, D. (2009) The origin of primary textures in granitic pegmatites. The Canadian Mineralogist, 47(4), 697-724.

London, D. (2014) A petrologic assessment of internal zonation in granitic pegmatites. Lithos, 184-187, 74-104.

London, D. (2015) Reply to Thomas and Davidson on “A petrologic assessment of internal zonation in granitic pegmatites” (London, 2014a). Lithos, 212–215, 469-484.

Mccreath, J.A., Finch, A.A., Herd, D.A., and Armour-Brown, A. (2013) Geochemistry of pyrochlore minerals from the Motzfeldt Center, South Greenland: The mineralogy of a syenite-hosted Ta, Nb deposit. American Mineralogist,

98(2-3), 426-438.

Morgan, VI G.B., London, D., (1996) Optimizing the electron microprobe analysis of hydrous alkali aluminosilicate glasses. American Mineralogist, 81(9-10): 1176-1185.

Morgan, VI G.B., and London, D. (2005) Phosphorus distribution between potassic alkali feldspar and metaluminous haplogranitic liquid at 200 MPa (H_2O): the effect of undercooling on crystal–liquid systematics. Contributions to Mineralogy and Petrology, 150(4), 456-471.

Mungall, J.E., Dingwell, D.B., and Chaussidon, M. (1999) Chemical diffusivities of 18 trace elements in granitoid melts. Geochimica et Cosmochimica Acta, 63(17), 2599-2610.

Mysen, B.O., Holtz, F., Pichavant, M., Beny, J.M., and Montel, J.M. (1997) Solution mechanisms of phosphorus in quenched hydrous and anhydrous granitic glass as a function of peraluminosity. Geochimica et Cosmochimica Acta, 61(18): 3913-3926.

Mysen, B.O., and Toplis, M.J. (2007) Structural behavior of Al3+ in peralkaline, metaluminous, and peraluminous silicate melts and glasses at ambient pressure. American Mineralogist, 92(5-6), 933-946.

Raimbault, L., Cuney, M., Azencott, C., Duthou, J.L., and Joron, J.L. (1995) Geochemical evidence for a multistage magmatic genesis of Ta-Sn-Li mineralization in the granite at Beauvoir, French Massif Central. Economic Geology, 90(3): 548-576.

473 Rao, C.Wang R.C., Frédéric, H., Gu, X.P., Ottolini, L., Hu, H., Dong C.W., Fabrice,
474 D.B., and Maxime, B. (2014) Strontiohurlbutite, SrBe2(PO4)2, a new mineral
475 from Nanping No. 31 pegmatite, Fujian Province, Southeastern China,
476 American Mineralogist, pp. 494.
477 Robie, R.A., Huebner, J.S., and Hemingway, B.S. (1995) Heat capacities and
478 thermodynamic properties of braunite (Mn7SiO12) and rhodonite (MnSiO3).
479 American Mineralogist, 80, 560-575.
480 Stilling, A., Černý, P., and Vanstone, P.J. (2006) the Tanco pegmatite at Bernic Lake,
481 Manitoba XVI. Zonal and bulk compositions and their petrogenetic
482 significance. The Candian Mineralogist, 44: 599-623.
483 Thomas, R., Webster, J.D., and Rhede, D. (1998) Strong phosphorus enrichment in a
484 pegmatite-forming melt. Acta Universitatis Carolinae–Geologica, 42, 150-164.
485 Thompson, L.M., and Stebbins, J.F. (2011) Non-bridging oxygen and
486 high-coordinated aluminum in metaluminous and peraluminous calcium and
487 potassium aluminosilicate glasses: High-resolution 17O and 27Al MAS NMR
488 results. American Mineralogist, 96(5-6), 841-853.
489 Toplis, M.J., and Dingwell, D.B. (1996) The variable influence of P_2O_5 on the
490 viscosity of melts of differing alkali/aluminium ratio: Implications for the
491 structural role of phosphorus in silicate melts. Geochimica et Cosmochimica
492 Acta, 60(21): 4107-4121.
493 Van Lichtervelde, M., Holtz, F., and Hanchar, J. (2010) Solubility of manganotantalite,
494 zircon and hafnon in highly fluxed peralkaline to peraluminous pegmatitic

melts. Contributions to Mineralogy and Petrology, 160(1): 17-32.

Watson, E.B. (1979) Zircon saturation in felsic liquids: Experimental results and applications to trace element geochemistry. Contributions to Mineralogy and Petrology, 70(4), 407-419.

Wolf, M., and London, D. (1993) Preliminary results of HFS and RE element solubility experiments in granites as a function of B and P. Eos, 74: 343.

Wolf, M.B., and London, D. (1994) Apatite dissolution into peraluminous haplogranitic melts: An experimental study of solubilities and mechanisms. Geochimica et Cosmochimica Acta, 58(19), 4127-4145.

Yin, L., Pollard, P.J., Shouxi, H., and Taylor, R.G. (1995) Geologic and geochemical characteristics of the Yichun Ta-Nb-Li deposit, Jiangxi Province, South China. Economic Geology, 90(3): 577-585.

Figure captions:

Fig.1 typical BSE imaging of run product. Mc=Mn-columbite, Mt= Mn-tantalite, and V=Vesicle

Fig.2 The effect of phosphorus on the solubility of Mn-columbite and Mn-tantalite at 800°C and 100 MPa

Fig.3 The effect of melt compositions on the solubility of Mn-columbite and Mn-tantalite. The data of Linnen and Keppler (1997) were plotted here for comparison. The more discussion of the P structural role is provided in text.

Fig.4 The effect of melt compositions (fluxing elements) on the solubility of Mn-columbite and Mn-tantalite. The data of Linnen and Keppler (1997) were plotted here for comparison. A P:M ratio of 1:1 is assumed (M=metal cations).

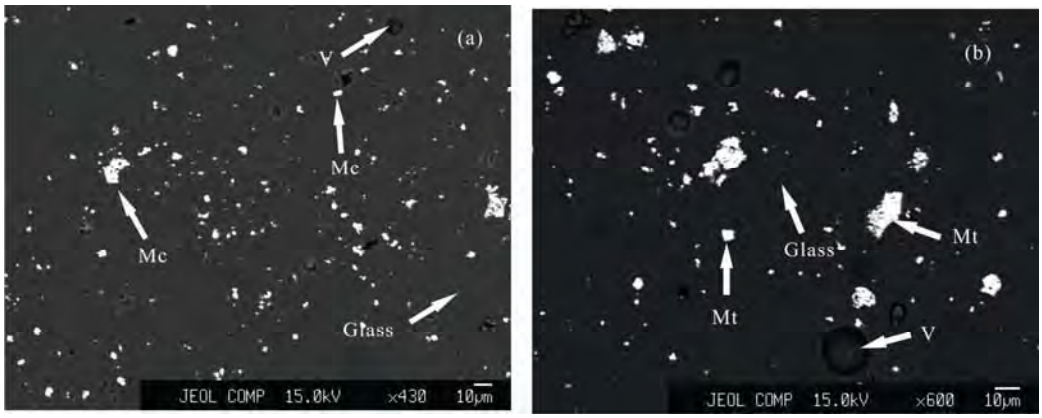
(a)
V
Me
Mc
Glass
JEOL COMP 15.0kV ×430 10μm
(b)
Glass
Mt
Mt
V
JEOL COMP 15.0kV ×600 10μm

FIGURE 1

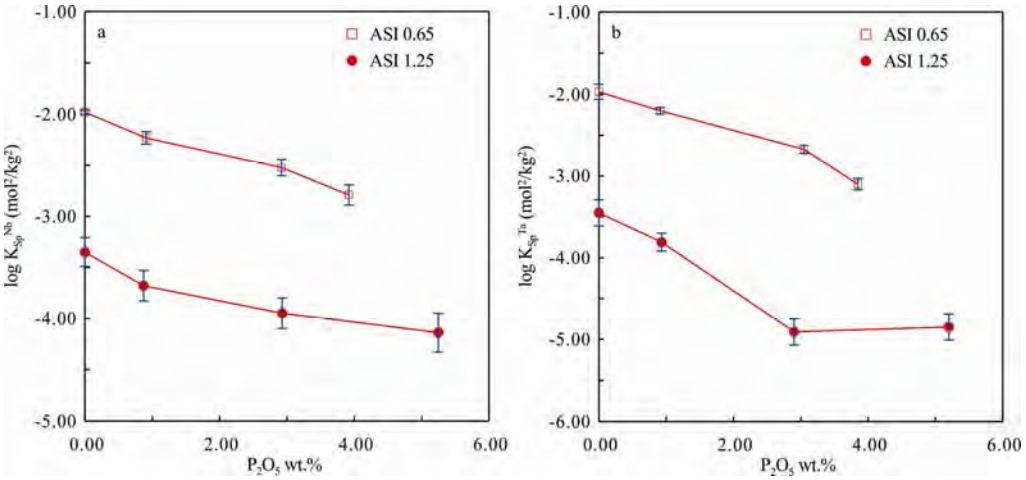
a
ASI 0.65
ASI 1.25
-1.00
-2.00
-3.00
-4.00
-5.00
0.00
2.00
4.00
6.00
P2O5 wt.%
b
ASI 0.65
ASI 1.25
-1.00
-2.00
-3.00
-4.00
-5.00
-6.00
0.00
2.00
4.00
6.00
P2O5 wt.%

FIGURE 2

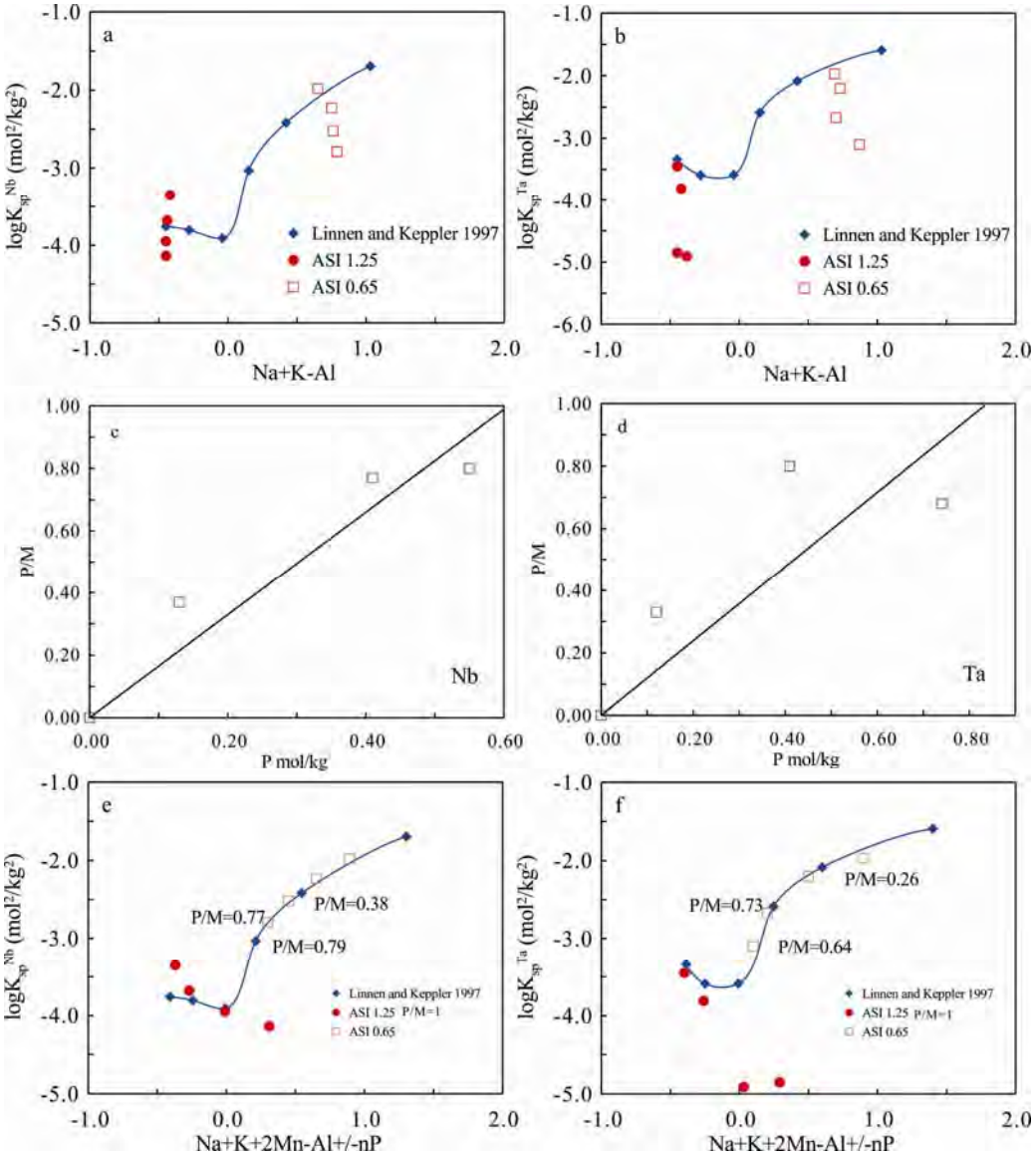
a
b
c
d
e
f
Linnen and Keppler 1997
ASI 1.25
ASI 0.65
Na+K-Al
P/M
P mol/kg
Nb
Ta
P/M=0.77
P/M=0.38
P/M=0.79
P/M=0.73
P/M=0.26
P/M=0.64
Na+K+2Mn-Al+/-nP

FIGURE 3

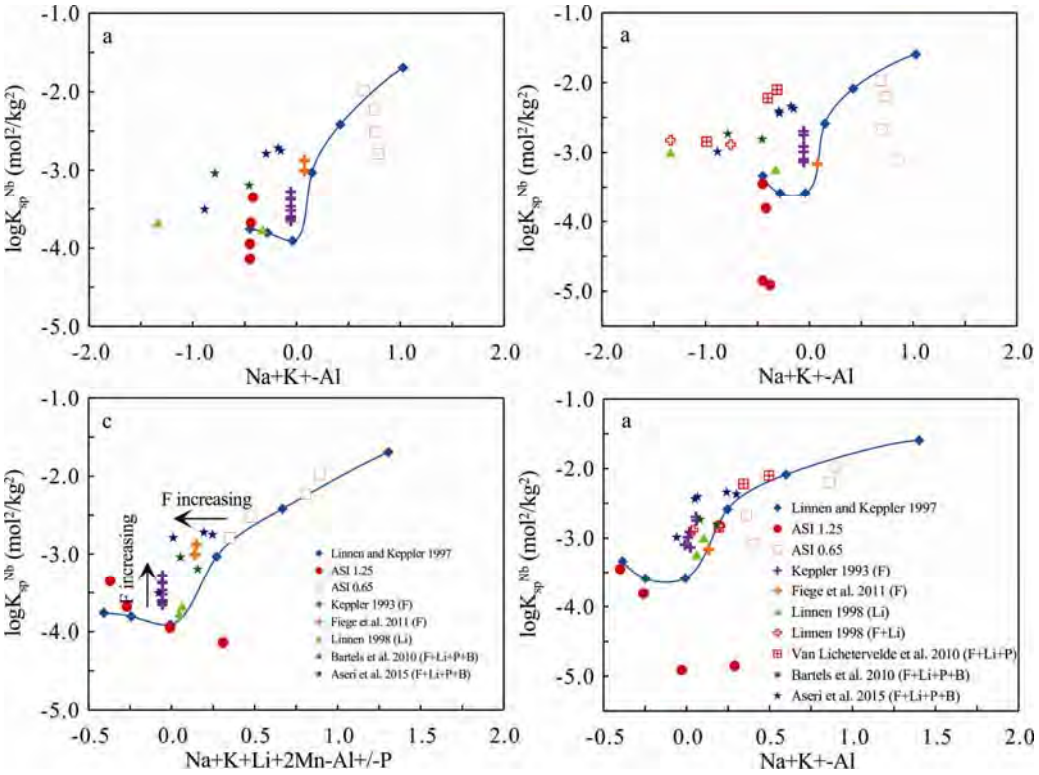
a
a
c
a
logK$_{sp}^{Nb}$ (mol^2/kg^2)
Na+K+-Al
Na+K+Li+2Mn-Al+/-P
F increasing
F increasing
Linnen and Keppler 1997
ASI 1.25
ASI 0.65
Keppler 1993 (F)
Fiege et al. 2011 (F)
Linnen 1998 (Li)
Linnen 1998 (F+Li)
Van Lichtervelde et al. 2010 (F+Li+P)
Bartels et al. 2010 (F+Li+P+B)
Aseri et al. 2015 (F+Li+P+B)

FIGURE 4

665
666
667
668
669
670
671
672
673
674
675 Table captions:
676
677 Table1. Chemical compositions of the initial glasses, determined by XRF (wt. %)
678 Table 2. Compositions of synthetic manganocolumbite and manganotantalite
679 Table 3. Experimental results of Mn-columbite and Mn-tantalite dissolution
680 experiments
681
682
683
684
685
686
687
688
689
690
691
692

693

694

695

696

697

698 Table1. Chemical compositions of the initial glasses, determined by XRF (wt. %)

Sample	SiO_2	Al_2O_3	Na_2O	K_2O	P_2O_5	total	ASI
HP-11-1	78.51	8.63	4.68	5.15	0.00	96.97	0.65
HP-11-2	77.44	9.11	5.33	4.94	1.11	97.93	0.65
HP-11-3	76.47	8.80	5.45	4.98	3.33	99.03	0.61
HP-11-4	75.35	8.71	5.21	4.68	4.23	98.18	0.64
HP-11-5	78.06	11.02	3.74	4.12	0.00	96.94	0.98
HP-11-6	77.82	11.78	3.36	3.72	0.00	96.68	1.23
HP-11-7	77.22	11.61	3.25	3.66	1.01	96.75	1.25
HP-11-8	77.28	11.43	3.18	3.56	3.19	98.64	1.26
HP-11-9	76.51	11.03	3.07	3.43	5.65	99.69	1.26

699 ASI= molar Al_2O_3/Na_2O+K_2O

700

701

702

703

704

Table 2 Compositions of synthetic Mn-columbite and Mn-tantalite

Crystal type	MnO (wt.%)	Nb_2O_5 or Ta_2O_5 (wt.%)	Mn/Nb or Mn/Ta	total
$MnNb_2O_6$	21.90(0.33)	77.97(0.69)	0.53(0.01)	99.87
$MnTa_2O_6$	13.37(0.98)	85.51(1.15)	0.49(0.04)	98.88

Table 3 Experimental results of Mn-columbite and Mn-tantalite dissolution experiments.

Run No.	sample	SiO_2	Al_2O_3	Na_2O	K_2O	H_2O*	ASI	EA mol/kg	EA_{Mn} mol/kg	EA_{Lk} mol/kg	ΔEA (mol/kg)	P_2O_5 (wt%)	P/M	MnO (wt%)	$(Nb, Ta)_2O_5$ (wt%)	Mn/(Nb, Ta)	$K_{Sp}^{(Nb, Ta)}$ ($10^{-4}mol^2/kg^2$)	$\log K_{Sp}^{(Nb, Ta)}$ (mol^2/kg^2)
Nb1	HP-11-1	75.82(0.29)	8.02(0.27)	3.93(0.17)	4.51(0.18)	4.53	0.71	0.65	0.89	/	0.00	0.00(0.00)	0	0.85(0.05)	2.33(0.08)	0.68(0.04)	104.89(6.55)	-1.98(0.02)
Nb2	HP-11-2	74.37(0.28)	8.63(0.15)	4.56(0.14)	4.57(0.22)	4.66	0.69	0.75	0.94	0.60	0.34	0.91(0.07)	0.38	0.68(0.11)	1.63(0.12)	0.78(0.14)	58.83(10.69)	-2.23(0.06)
Nb3	HP-11-3	73.97(0.33)	8.23(0.25)	4.37(0.25)	4.54(0.20)	4.29	0.68	0.76	0.89	0.35	0.54	2.92(0.05)	0.77	0.46(0.10)	1.22(0.15)	0.71(0.17)	29.95(7.20)	-2.52(0.08)
Nb4	HP-11-4	73.59(0.33)	7.83(0.28)	4.43(0.19)	4.43(0.19)	4.81	0.66	0.79	0.90	0.20	070	3.92(0.07)	0.79	0.38(0.08)	0.80(0.15)	0.89(0.26)	16.11(4.65)	-2.79(0.10)
Nb5	HP-11-6	77.57(0.36)	10.55(0.33)	2.95(0.11)	3.30(0.18)	4.98	1.25	-0.42	-0.37	/	/	0.00(0.00)	1/1	0.18(0.06)	0.47(0.13)	0.72(0.30)	4.50(1.85)	-3.35(0.14)
Nb6	HP-11-7	75.92(0.36)	11.05(0.35)	3.13(0.13)	3.39(0.13)	5.22	1.25	-0.44	-0.40	/	/	0.87(0.04)	1/1	0.14(0.05)	0.28(0.09)	0.95(0.43)	2.07(0.93)	-3.68(0.15)
Nb7	HP-11-8	74.97(0.27)	10.71(0.31)	2.99(0.11)	3.23(0.16)	4.85	1.27	-0.45	-0.42	/	/	2.93(0.09)	1/1	0.10(0.03)	0.21(0.06)	0.87(0.38)	1.12(0.49)	-3.95(0.15)
Nb8	HP-11-9	73.36(0.34)	10.48(0.24)	2.91(0.10)	3.15(0.08)	4.61	1.28	-0.45	-0.43	/	/	5.25(0.12)	1/1	0.08(0.01)	0.18(0.06)	0.82(0.45)	0.73(0.40)	-4.14(0.19)
Ta1	HP-11-1	74.33(0.20)	7.77(0.32)	3.89(0.14)	4.51(0.20)	4.20	0.69	0.69	0.90	/	0.00	0.00(0.00)	0	0.74(0.19)	4.55(0.24)	0.51(0.14)	107.62(28.84)	-1.97(0.09)
Ta2	HP-11-2	74.51(0.40)	8.16(0.26)	4.43(0.24)	4.26(0.15)	4.60	0.69	0.73	0.99	0.50	0.49	0.91(0.19)	0.26	0.89(0.09)	2.24(0.13)	1.24(0.15)	63.65(7.75)	-2.20(0.04)
Ta3	HP-11-3	72.79(0.31)	8.43(0.27)	4.39(0.20)	4.41(0.23)	4.55	0.70	0.70	0.79	0.20	0.59	3.05(0.09)	0.73	0.32(0.04)	2.08(0.07)	0.49(0.07)	21.49(2.90)	-2.67(0.05)
Ta4	HP-11-4	73.81(0.41)	7.57(0.28)	4.41(0.27)	4.40(0.21)	4.70	0.63	0.87	0.94	0.10	0.84	3.85(0.20)	0.64	0.24(0.04)	1.06(0.14)	0.70(0.14)	7.96(1.60)	-3.10(0.07)
Ta5	HP-11-6	77.26(0.40)	10.72(0.41)	2.82(0.11)	3.51(0.19)	4.82	1.25	-0.45	-0.40	/	/	0.00(0.00)	1/1	0.16(0.05)	0.70(0.25)	0.70(0.33)	3.57(1.70)	-3.45(0.16)
Ta6	HP-11-7	76.27(0.29)	10.76(0.23)	3.09(0.13)	3.26(0.14)	5.17	1.25	-0.42	-0.39	/	/	0.93(0.07)	1/1	0.12(0.03)	0.40(0.07)	0.93(0.29)	1..55(0.48)	-3.81(0.11)
Ta7	HP-11-8	74.75(0.36)	10.51(0.31)	3.09(0.12)	3.23(0.14)	5.34	1.22	-0.38	-0.37	/	/	2.90(0.10)	1/1	0.02(0.01)	0.16(0.04)	0.48(0.22)	0.12(0.06)	-4.91(0.16)
Ta8	HP-11-9	73.20(0.24)	10.47(0.22)	2.90(0.09)	3.16(0.8)	4.87	1.28	-0.45	-0.44	/	/	5.20(0.08)	1/1	0.03(0.01)	0.16(0.03)	0.56(0.25)	0.14(0.07)	-4.85(0.16)
Ta9	HP-11-5	76.65(0.29)	10.41(0.33)	3.65(0.12)	4.02(0.10)	4.46	1.00	-0.01	0.04	/	/	0.00(0.00)	0	0.17(0.03)	0.65 (0.17)	0.83(0.27)	3.54(1.15)	-3.45 (0.11)
Ta9[1]	HP-11-5	76.77(0.33)	10.47(0.40)	3.66(0.09)	4.08(0.10)	4.21	1.00	-0.01	0.04	/	/	0.00(0.00)	0	0.15(0.02)	0.65(0.10)	0.74(0.16)	3.16(0.67)	-3.50 (0.07)

ASI is the molar ratio Al/(Na+K) o; EA equals the molar Na+K-Al per kilogram; EA_{Mn} is the molar Na+K+Li+2*Mn-Al per kilogram; EA_{LK} is the value that coincides with the reference curve of Linnen and Keppler (1997); $\Delta EA = EA_{Mn}\text{-}EA_{LK}$; / is not reference point or not calculated; M is Na, K, and Mn in the present work. P/M= P (mol/kg)/ΔEA (mol/kg). The duration time of all experiments is 10 days, except for TA9[1] (16days). The water contents (H_2O*) of the glass were estimated based on difference of EMPA oxide totals from 100%.